Hindawi Publishing Corporation
International Journal of Photoenergy
Volume 2008, Article ID 827605, 7 pages
doi:10.1155/2008/827605

Research Article

Studies of Dye Sensitisation Kinetics and Sorption Isotherms of Direct Red 23 on Titania

Peter J. Holliman,[1] Beatriz Vaca Velasco,[1] Ian Butler,[1] Maarten Wijdekop,[2] and David A. Worsley[3]

[1] *School of Chemistry, Bangor University, Gwynedd LL57 2UW, UK*
[2] *Corus Colors, Shotton Works, Flintshire CH5 2 NH, UK*
[3] *School of Engineering, Swansea University, Swansea SA2 8PP, UK*

Correspondence should be addressed to Peter J. Holliman, p.j.holliman@bangor.ac.uk

Received 27 March 2008; Revised 27 March 2008; Accepted 19 May 2008

Recommended by Russell Howe

Sorption kinetics and isotherms have been measured for a commercial dye (Direct Red 23) on different samples of powdered Titania, and the data were analysed to better understand the dye sensitization process for dye sensitised solar cells (DSSCs). For the sorption kinetics, the data show rapid initial sorption (<1 hour) followed by slower rate of increasing uptake between 1 and 24 hours. While higher initial concentrations of dye correspond to higher sorption overall, less dye is absorbed from higher initial dye concentrations when considered as percentage uptake. The correlation between the sorption data and model isotherms has been considered with time. The Langmuir model shows better correlations compared to the Freundlich isotherm. The dye uptake data has also been correlated with Titania characterization data (X-ray diffraction, scanning electron microscopy, BET and zero point charge analysis). Kinetic data show significantly better fits to second-order models compared to first order. This suggests that chemisorption is taking place and that the interaction between the dye sorbate and the Titania sorbent involves electron sharing to form an ester bond.

1. INTRODUCTION

The need for commercially viable renewable energy sources such as photovoltaic (solar cell) devices is increasing in line with concerns over climate change resulting from fossil fuel combustion [1]. Dye sensitised solar cells (DSSCs) have the advantage that this is a relatively low-cost photovoltaic technology [2]. A DSSC device uses a dye chemisorbed to an oxide semiconductor such as Titania and operates by the dye reaching an excited state by absorbing photons in the visible region and injecting these electrons into the oxide. The electrons then pass between TiO_2 particles to an electrode and around a circuit to a second electrode finally passing via an electrolyte back to the dye to continue the cycle.

A major breakthrough in DSSC technology (solar efficiency 7%) was achieved by O'Regan and Grätzel in 1991 [3] using a Ru bipyridyl complex (the N3 dye) as the dye sensitizer along with high-surface area nanoparticulate Titania. Subsequent work by Grätzel and coworkers to develop new dyes has resulted in increased solar efficiencies for DSSC (up to 10.4%) using N719 [4] and Ru terpyridyl "black dye" [5]. Since 1991, a great deal of work has been carried out on studying new dyes as sensitizers to optimise extinction coefficient, rates of electron injection into TiO_2, and rates of regeneration of the ground state dye by interaction with the electrolyte [6, 7]. While ruthenium(II)bipy complexes have by far been the most widely studied dyes for DSSC, more recently, indoline [8], unsymmetrical phthalocyanines [9], and squaraine dyes [10] have also been reported as showing promise.

Typically, Titania is sensitized by soaking the oxide in a dye solution for either a period of hours or even overnight. However, to scale up the manufacture of DSSC, dyes must meet materials processing criteria, one of which is that the dye sensitisation process needs to take place more rapidly. In this context, the adsorption and desorption behavior of the Ru dye N3 has been studied stressing that dye coverage above 0.3 of a monolayer is necessary to increase current efficiency [11]. Also working on Ru dyes, Nazeeruddin et al. have reported a swift uptake procedure for the N719 dye [12]. More recently, it has been reported that electron injection rates into the metal oxide are an order of magnitude slower

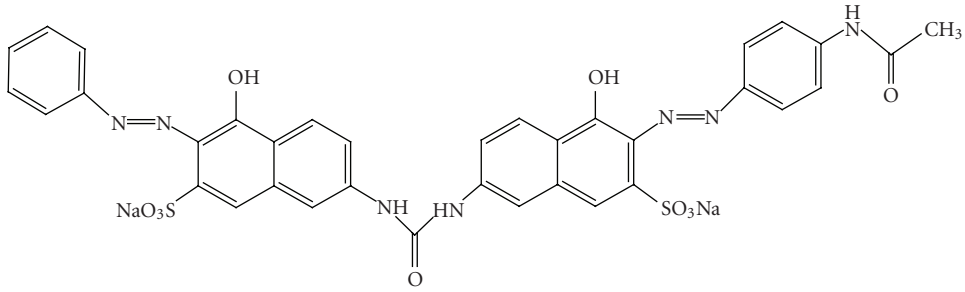

Figure 1: Chemical structure of the commercial diazo dye Direct Red 23 (C.I. 29160).

for aggregated dye compared with monomeric sensitizer dye emphasising the need for efficient monolayer sensitization [13].

This paper investigates the sorption isotherms and kinetics for the commercially available azo dye Direct Red 23 on different samples of Titania and correlates these data with both model isotherms and the physicochemical characteristics for the Titania samples. These data have been used to develop a clearer understanding of the dye sensitization process when considering time and dye concentration as two key variables.

2. EXPERIMENTAL

Three variables were explored using the commercial azo dye Direct Red 23, C.I. 29160 (Aldrich); TiO_2 grade (four samples labelled A to D were used), dye concentration (from 163 mg l^{-1} to 650 mg l^{-1}), and time (up to 24 hours).

Sorption experiments were carried out using two replicates. The data were averaged and the standard errors are shown in Figures 2(b) and 2(c). In a typical experiment, methanol (50 mL, HPLC grade, Aldrich) containing the appropriate dye concentration was added to titanium dioxide powder (1 g) in a 50 mL flask, shaken for 1 minute and left to stand. Aliquots (1.5 mL) were taken after 15, 30, and 60 minutes, then every 1 hour up to 8 hours and then at 23 and 24 hours. These were centrifuged for 10 minutes at 8000 rpm before the solution dye concentration was measured by UV-visible spectroscopy at $\lambda = 500$ nm. If necessary, dilution was carried out (1 mL in 10 mL of methanol). The amount of sorption (mg kg^{-1}) was calculated as the difference between the amount of dye initially added and that measured at each measurement time. Langmuir (1) and Freundlich (2) and (3) sorption isotherm equations were fitted to the experimental data by a computerized least-squares optimization routine, where

$$\frac{C_e}{q_e} = \frac{1}{Q_0 b} + \frac{C_e}{Q_0} \quad \text{(see, [14])} \tag{1}$$

$$q_e = k_f \times C_e^{1/n} \tag{2}$$

$$\log_{10} q_e = \log_{10} k_F + \frac{1}{n}\log_{10} C_e, \quad \text{(see, [15])}, \tag{3}$$

where C_e is the concentration of dye in the solution (mg l^{-1}) at equilibrium, q_e is the dye concentration adsorbed onto the TiO_2 (mg g^{-1}) at equilibrium, and Q_0 (mg g^{-1}) and b (l mg^{-1}) are constants related to the adsorption capacity and to the energy of adsorption, respectively [14]. For the Freundlich isotherm, k_F is a constant which measures the adsorption capacity and $1/n$ is a measure of the adsorption intensity [15]. The values for k_F and n were calculated from the intercept and slope of the plots. The solid-to-solution partition coefficient (K_d) was determined from the following equation

$$K_d = \frac{C_{\text{tot}}}{C_e}, \tag{4}$$

where C_{tot} is the total dye ($C_e + q_e$).

For TiO_2 samples A and C, first- and second-order kinetic equations were fitted to the data according to the equations proposed by Kannan and Sundaram (5) [16] and Ho and McKay (6) [17], respectively,

$$\frac{1}{q_t} = \left(\frac{k}{q_{\max}}\right)\left(\frac{1}{t}\right) + \frac{1}{q_{\max}} \quad \text{(see, [16])} \tag{5}$$

$$\frac{t}{q} = \frac{1}{k_2 q_e^2} + \frac{t}{q_e} \quad \text{(see, [17])}. \tag{6}$$

For the first-order model (5), q_t is the amount of dye adsorbed in mg g^{-1} at various times (t), $q_{\max}$ is the maximum adsorption capacity, and k is the first-order rate constant in min^{-1} [16]. Linear correlation of $1/q_t$ versus $1/t$ was made to samples A and C at 3 different dye concentrations. For the second-order model, the initial adsorption rate h in mg g^{-1} min^{-1} can be defined as $h = k_2 q_e^2$, where q_e is the equilibrium adsorption capacity in mg g^{-1} and k_2 is the second-order constant in g mg^{-1} min [17]. Both variables were calculated from the slope and intercept, respectively.

2.1. Characterisation techniques

X-ray powder diffraction (XRD) data was measured between 5 and 75 degrees two theta using Ni-filtered Cu Kα1 radiation ($\lambda = 1.54051$ Å) on an X'Pert PRO theta-theta diffractometer (PANalytical Ltd) at 45 kV and 35 mA.

Gold sputtered samples were analyzed by scanning electron microscopy (SEM) at 11 kV on a Hitachi S-520 SEM. EDAX was measured on the same instrument at 14 kV with an Oxford Instruments 7497 EDAX with Link ISIS computer software.

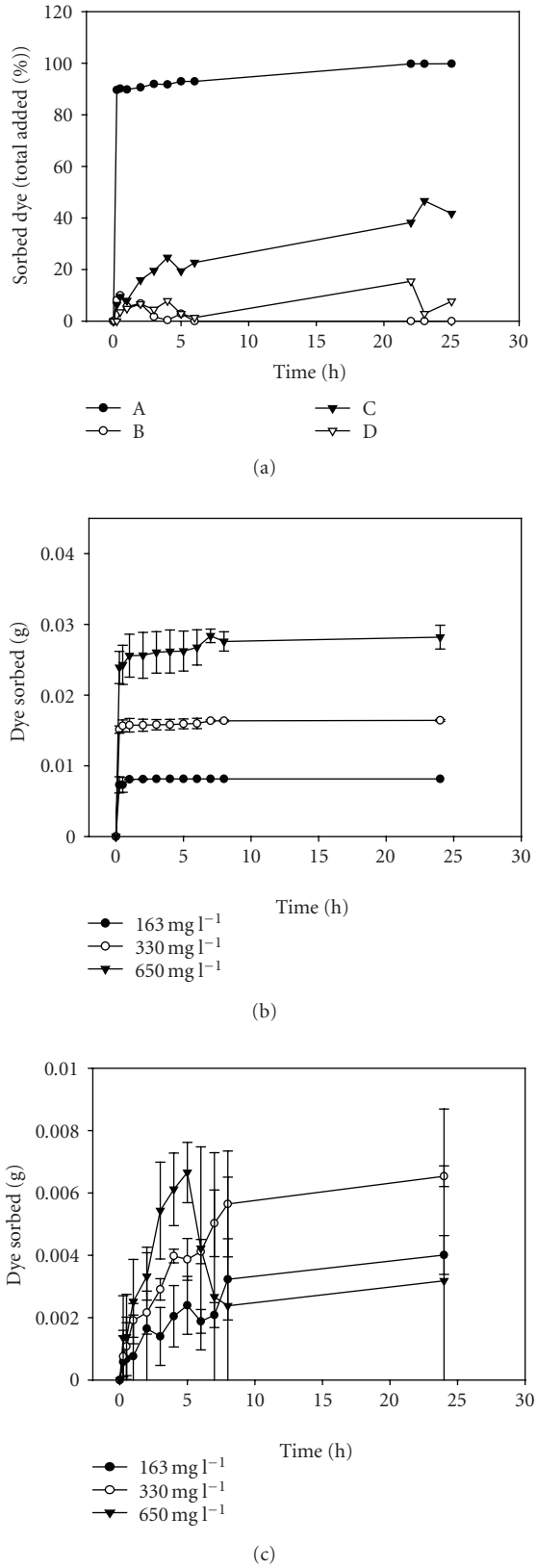

Figure 2: Sorption kinetics of (a) 330 mg l^{-1} of Direct Red 23 onto four different samples of TiO_2; (b) varying concentrations of Direct Red 23 onto TiO_2 sample A; (c) varying concentrations of Direct Red 23 onto TiO_2 sample C. Error bars are omitted from (a) for clarity.

The surface areas of the TiO_2 powders were measured at 77 K on a Micrometrics Gemini III 2375 and the data analyzed using BET (Braumer, Emmet, and Teller) isotherms.

Zero point charge (ZPC) was determined by the salt-addition method [18] using three replicates. In the procedure, ten aliquots of 0.1 M $NaNO_{3(aq)}$ (40 mL, Aldrich) were adjusted to varying pH between 2 and 11 using $NaOH_{(aq)}$ (99.99%, Aldrich) or $HNO_{3(aq)}$ (Aldrich). TiO_2 (0.2 g) was added to each aliquot, thoroughly mixed, and the pH measured after 24 hours. The difference between final pH and initial pH (ΔpH) was plotted against initial pH. ZPC was then calculated from this graph at the point where ΔpH = 0.

UV-visible spectroscopy was measured in silica cuvettes (1 cm path length) on an ATI UNICAM UV4 spectrometer and the data analyzed using VisionScan software. The instrument was calibrated using inhouse standards from 0 to 200 mg l^{-1} (typical equation was $y = 37200x - 0.004$ with $R^2 > 0.99$).

3. RESULTS AND DISCUSSION

3.1. TiO_2 powder characterisation

Four commercial samples of Titania powder have been investigated. Sample A is Degussa P25, an uncoated nanoparticulate Titania; sample B is Kronos 1001 an uncoated, anatase pigment grade Titania; sample C is Kronos 2063; and sample D is Kronos 2220, a coated rutile pigment grade Titania.

X-ray powder diffraction data (Table 1) show that Sample A is a mixture of *ca.* 80% anatase [19] and 20% rutile [20].The diffraction peaks are broader than the other samples reflecting the smaller particle size range which is confirmed by electron microscopy. Sample B shows only anatase along with narrower diffraction lines suggesting larger particles. Samples C and D also exhibit narrower diffraction peaks more characteristic of larger particles. However, for both samples, rutile is the major phase.

Scanning electron microscopy shows that all the samples are made up of spherical particles with the main morphological difference between samples being particle size. Thus, sample A has the smallest particles (20–50 nm), the particles in samples B and C are 200–300 nm while those in D are 300–500 nm. Table 1 shows that the surface areas of samples B, C, and D are all broadly similar at 11 to 15 $m^2\,g^{-1}$ while sample A has a much higher surface area at *ca.* 50 $m^2\,g^{-1}$. Similarly, sample A differs from the others with a value for the zero point charge (ZPC) of 4.50 compared to samples B and C (both *ca.* 6.50) while sample D could not be measured due to problems dispersing this powder in water.

3.2. Sorption kinetics and Isotherms

Direct Red 23 is a commercial, azo dye containing two sulfonate groups (Figure 1) which can interact with O–H groups on the surface of Titania. The % sorption against time for an initial concentration of 330 mg l^{-1} of Direct Red 23 onto four samples of Titania are shown in Figure 2(a). For sample A, the data show very fast uptake of the majority of

Table 1: Selected characteristics of titania samples.

	Titania samples			
	A	B	C	D
Surface area ($m^2\ g^{-1}$)*	49.8 (1.5)	11.1 (0.7)	14.9 (0.3)	11.1 (0.4)
Particle size† (nm)	20–50	200–300	200–300	300–500
Zero point charge (ZPC)	4.50 (0.00)	6.50 (0.15)	6.40 (0.15)	Not measured
X-ray diffraction data	Anatase (80%) + Rutile (20%)	Anatase	Rutile	Rutile

*Standard deviation shown in parentheses.
†Average particle size measured by scanning electron microscopy.

Table 2: Langmuir and Freundlich isotherm data and partition coefficients for TiO_2 samples A and C at 1, 5, and 24 hours. For R^2, the range of values is shown from the replicate experiments. For other parameters, the data shown are averages with standard errors in parentheses.

		TiO_2 Sample A			TiO_2 Sample C		
		1 h	5 h	24 h	1 h	5 h	24 h
Langmuir	R^2	0.94–0.99	0.99	0.94–0.99	0.73-0.74	0.17–0.24	0.97-0.98
	Q_o	28.4 (2.8)	27.5 (4.9)	35.2 (5.3)	2.2 (0.0)	9.4 (1.5)	8.0 (0.2)
	b	0.37 (0.30)	0.37 (0.16)	0.91 (0.44)	−0.06 (0.01)	0.01 (0.00)	0.04 (0.01)
Freundlich	R^2	0.87–0.91	0.55–0.77	0.91–0.93	0.64–0.87	0.55–0.61	0.77–0.91
	K_f	11.5 (2.8)	13.5 (1.0)	15.3 (1.8)	0.5 (0.0)	0.6 (0.2)	1.0 (0.1)
	n	4.55 (0.51)	6.53 (2.48)	3.91 (1.72)	3.35 (0.12)	2.43 (0.50)	2.72 (0.00)
Dye conc.							
K_d	A:−200 mg l^{-1} C:−240 mg l^{-1}	278	423	1085	1.3	1.3	2.7
	640 mg l^{-1}	13	12	51	1.0	2.4	1.3

the dye during the first 15–30 minutes. This is followed by a much more gradual uptake of dye between 0.5 and 24 hours. Sample C shows the next fastest and highest dye uptake but this is much more gradual. However, there is more rapid dye uptake initially (in this case, 0–5 hours) and then a slower rate up to 24 hours. Finally, Samples B and D show little dye uptake (< 20%) with sample B showing evidence of sorption in the first few hours followed by desorption between 3 and 24 hours.

Figure 2(b) shows the effect on the rate of dye uptake of changing the initial dye concentration for Titania sample A. For 163 mg l^{-1}, almost all the dye is sorbed after 1 hours whilst for 330 mg l^{-1} and 650 mg l^{-1} dye uptake is still increasing up to *ca.* 8 hours. By comparison, Figure 2(c) shows the corresponding data for sample C. Here, the larger errors reflect the lower dye uptake compared to sample A and indeed the low uptake and large errors make further analysis of samples B and D impossible. However, for sample C, the data do show similar trends to sample A of slower and proportionally lower uptake of dye with increasing initial dye concentration. These data would seem to indicate that dye uptake becomes less favourable as the oxide surface becomes increasingly populated with sorbed dye molecules and solution dye concentrations decrease as might be expected.

Table 2 shows the results of fitting the sorption data to the Langmuir and Freundlich isotherm models after 1, 5, and 24 hours of sorption. The calculations are only shown for samples A and C because, as mentioned above, the dye uptake on samples B and D is so low. For both samples A and C, the R^2 values are generally better after 1 hour and then 24 hours; the increased scatter observed after 5 hours suggesting some surface reorganisation after initial dye sorption. For sample A, in all cases, there is a closer fit from the regression lines to the Langmuir isotherm (e.g., R^2 ranges from 0.94 to 0.99 for Langmuir but from 0.55 to 0.93 for the Freundlich isotherm). By comparison, sample C shows slightly better fits to the Freundlich isotherm at 1 and 5 hours (R^2 ranging from 0.55 to 0.87 compared to 0.17 to 0.74 for Langmuir) but, conversely, a better fit to Langmuir at 24 hours (R^2 is 0.97 to 0.98 compared to 0.77 to 0.91 for Freundlich). The Langmuir isotherm assumes monolayer coverage of sorbent but also that all the sorption sites are identical and that there is no interaction between sorbent molecules [21]. By comparison, the Freundlich isotherm assumes that the enthalpy of adsorption decreases exponentially with coverage [22]. The data show that the Langmuir model fits much more closely to the experimental data for this dye for sample A and sample C at equilibrium.

Thus a mechanism of sorption can be envisaged whereby, for the pristine oxide surface, the largest number of vacant sorption sites are available and the initial rate of dye uptake is quite rapid (Figure 2). For sample A, this results in almost quantitative dye sorption in equilibrium with very low dye concentration in the surrounding solution. However, as the sorption sites are filled, fewer vacant sorption sites remain and relatively more dye molecules remain in solution. This can be represented quite clearly when considering how the partition coefficient (K_d) varies with time. For instance, at lower dye concentrations, there is a trend towards increasing

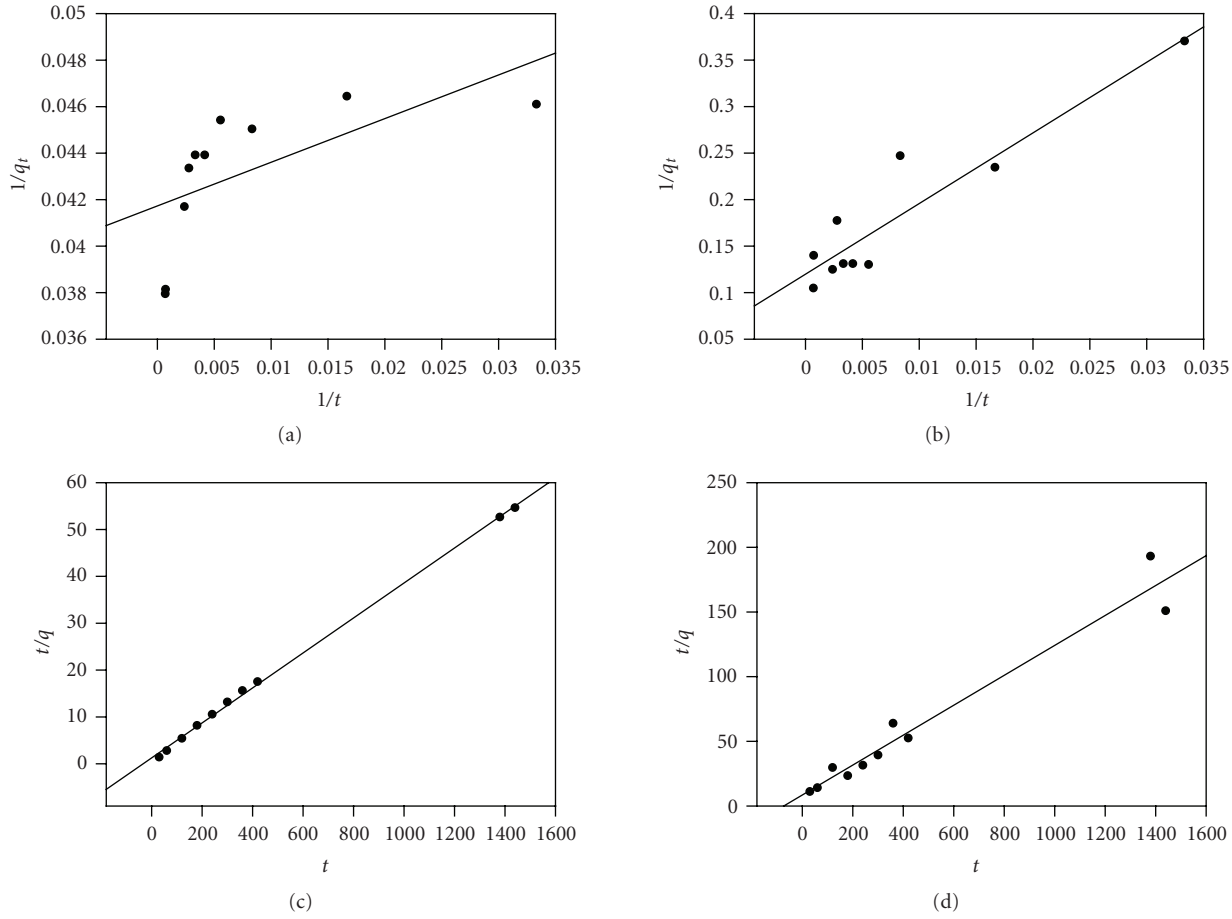

FIGURE 3: Kinetic plots at initial dye concentration of 650 mg l^{-1}. First-order plots for (a) sample A and (b) sample C. Second order plots for (c) sample A and (d) sample C.

K_d with time. Thus, for sample A, at 200 mg l^{-1}, K_d increases from 278 to 423 to 1085. This corresponds to an increasing proportion of dye sorbing to Titania compared to that remaining in solution. By comparison, although there is still an increase, K_d remains more constant at the higher dye concentrations (640 mg l^{-1}) for sample A. Overall, comparing samples A and C after 24-hour equilibration time, K_d ranges from 51 to 1085 for sample A but from 1 to 2.7 for sample C emphasizing that the equilibrium between sorbed and dissolved dye is hugely in favor of sorption for sample A across a range of dye concentrations but is much more evenly balanced for sample C (particularly at higher initial dye concentrations). Table 2 also shows that the Langmuir coefficients (Q_o and b) are larger for samples A compared with sample C which corresponds with the much greater dye uptake for the former over the latter.

Comparing all the sorption data with the characterisation data for the different Titania samples (Table 1) suggests that dye uptake is strongly influenced by metal oxide surface area and zero point charge. Most importantly, the higher surface area of sample A appears directly related to the increased uptake of this oxide because this presents a larger number of sorption sites which would be expected to lead to increased dye uptake. In addition, although the number of samples is relatively small, the data suggest that a lower value of zero point charge (ZPC) such as in sample A is an advantage. This implies that Titania sample A has a deprotonated surface at lower pH than Titania samples B and C. This is important if the mechanism of dye uptake is ascribed to chemisorption of the dyes to the Titania via the formation of sulfonate ester linkages between dye and surface O–H groups on the oxide with associated loss of water. Thus, the chemisorption process can be envisaged as occurring by nucleophilic attack of O–H groups from the Titania at the sulphur atom of the sulfonate group of the dye to forming the ester linkage. This suggests that deprotonation of the surface would lead to stronger nucleophiles which would enhance this process leading to more favourable uptake for sample A.

4. DYE SORPTION KINETICS

The results of the modelling of the kinetic data are shown in Table 3 with selected graphs in Figure 3. The data show that the linear regressions are poorer for the first-order kinetic model compared to the second-order data particularly for sample A (first-order R^2 ranges from 0.09 to 0.90 compared to 0.99 to 1.00 for second order) across the three different concentrations studied. This suggests a second-order kinetic

Table 3: Kinetic parameters for Direct Red 23 uptake onto TiO_2 samples A and C. For R^2, the range of values is shown from the replicate experiments. For other parameters, the data shown are averages with standard errors in parentheses.

		A			C		
C_o (mg l^{-1})		163	330	650	163	330	650
1st order	R^2	0.09–0.91	0.33–0.74	0.39–0.90	0.65–0.78	0.47–0.93	0.87–0.98
	K	2.42 (2.41)	1.15 (0.55)	2.97 (1.29)	19.1 (19.1)	91.4 (47.9)	295 (470)
	q_{max}	8.2 (0.1)	16.0 (0.6)	26.8 (2.8)	3.7 (3.7)	4.6 (0.3)	12.1 (9.5)
2nd order	R^2	0.99-1.00	0.99-1.00	0.99	0.07–0.99	0.90–0.97	0.60–0.95
	K_2	1.14 (1.75)	0.03 (0.03)	0.003 (0.002)	0.06 (0.06)	0.002 (0.002)	0.001 (0.001)
	q_e	8.1 (0.1)	16.5 (0.1)	28.3 (1.6)	5.5 (6.0)	7.9 (0.7)	12.9 (4.3)
	h	73 (112)	8 (10)	3 (2)	0.02 (0.04)	0.03 (0.01)	0.08 (0.05)

process dominates Direct Red 23 adsorption onto these Titania samples. This suggests that the rate-limiting step is a chemisorption process where sharing or exchange electrons between sorbent and sorbate takes place. In this case, the likelihood is that a sulfonate ester bond forms between the sulfonate groups on the dye and surface hydroxyl groups in the Titania.

Sample A produced the highest values for the parameters in the second-order kinetics equation (Table 3). Comparing the data for the initial adsorption rate (hour), these are the highest at the lowest dye concentration, decreasing dramatically as the initial dye concentration increases. This suggests that the kinetics of adsorption to the most energetically available adsorption sites are much faster and that as coverage increases, the rate of adsorption slows when only less energetically favorable sites remain. This gives a different insight into the adsorption process compared to the sorption isotherms (Langmuir) which reflect much more an equilibrium situation.

5. CONCLUSIONS

Dye sensitization is a key process in the manufacture of dye sensitized solar cell devices with very rapid dyeing uptake leading to full-monolayer coverage representing optimum objectives. Closely linked to these are the requirements for large amounts of dye uptake to maximize light absorption allowing for thinner devices along with a need for strongly chemisorbed dye molecules which do not desorb under device working conditions. The data presented for sorption of Direct Red 23 onto Titania sample A (Degussa P25) do show some of these characteristics and this is believed to be related to the higher surface area of this material along with a lower value of ZPC which offer a greater number of sorption sites and a more favourable sites for chemisorption of the dye, respectively.

Finally, whilse Direct Red 23 is not used in the currently, most efficient dye sensitized solar cells, this commercially available dye does possess similar anionic groups for adsorption onto Titania compared to Ru complexes and organic dyes. Thus, the data presented have important implications for dye sensitisation especially in the context of growing interest in organic dyes for DSSC.

ACKNOWLEDGMENTS

We gratefully acknowledge EU (ESF) Objective One funding and Corus support for BVV, Dr. Callum Hill for BET data, and Steve Jones for collecting the XRD data.

REFERENCES

[1] S. S. Hegedus and A. Luque, "Status, trends, challenges and the bright future of solar electricity from photovoltaics," in *Handbook of Photovoltaic Science and Engineering*, A. Luque and S. S. Hegedus, Eds., p. 177, John Wiley & Sons, Chichester, UK, 2003.

[2] K. Hara and H. Arakawa, "Dye-sensitized solar cells," in *Handbook of Photovoltaic Science and Engineering*, A. Luque and S. S. Hegedus, Eds., John Wiley & Sons, Chichester, UK, 2003.

[3] B. O'Regan and M. Grätzel, "A low-cost, high-efficiency solar cell based on dye-sensitized colloidal TiO_2 films," *Nature*, vol. 353, no. 6346, pp. 737–740, 1991.

[4] M. K. Nazeeruddin, A. Kay, I. Rodicio, et al., "Conversion of light to electricity by *cis*-X_2bis(2,2′-bipyridyl-4,4′-dicarboxylate)ruthenium(II) charge-transfer sensitizers (X = Cl^-, Br^-, I^-, CN^-, and SCN^-) on nanocrystalline TiO_2 electrodes," *Journal of the American Chemical Society*, vol. 115, no. 14, pp. 6382–6390, 1993.

[5] M. K. Nazeeruddin, P. Péchy, and M. Grätzel, "Efficient panchromatic sensitization of nanocrystalline TiO_2 films by a black dye based on a trithiocyanato-ruthenium complex," *Chemical Communications*, no. 18, pp. 1705–1706, 1997.

[6] N. Robertson, "Optimizing dyes for dye-sensitized solar cells," *Angewandte Chemie International Edition*, vol. 45, no. 15, pp. 2338–2345, 2006.

[7] R. Katoh, A. Furube, A. V. Barzykin, H. Arakawa, and M. Tachiya, "Kinetics and mechanism of electron injection and charge recombination in dye-sensitized nanocrystalline semiconductors," *Coordination Chemistry Reviews*, vol. 248, no. 13-14, pp. 1195–1213, 2004.

[8] T. Horiuchi, H. Miura, and S. Uchida, "Highly-efficient metal-free organic dyes for dye-sensitized solar cells," *Chemical Communications*, vol. 9, no. 24, pp. 3036–3037, 2003.

[9] P. Y. Reddy, L. Giribabu, C. Lyness, et al., "Efficient sensitization of nanocrystalline TiO_2 films by near-IR-absorbing unsymmetrical zinc phthalocyanine," *Angewandte Chemie*, vol. 119, no. 3, pp. 377–380, 2007.

[10] A. Burke, L. Schmidt-Mende, S. Ito, and M. Grätzel, "A novel blue dye for near-IR 'dye-sensitised' solar cell applications," *Chemical Communications*, no. 3, pp. 234–236, 2007.

[11] A. Fillinger and B. A. Parkinson, "The adsorption behavior of a ruthenium-based sensitizing dye to nanocrystalline TiO_2 coverage effects on the external and internal sensitization quantum yields," *Journal of the Electrochemical Society*, vol. 146, no. 12, pp. 4559–4564, 1999.

[12] M. K. Nazeeruddin, R. Splivallo, P. Liska, P. Comte, and M. Grätzel, "A swift dye uptake procedure for dye sensitized solar cells," *Chemical Communications*, vol. 9, no. 12, pp. 1456–1457, 2003.

[13] S. Tatay, S. A. Haque, B. O'Regan, et al., "Kinetic competition in liquid electrolyte and solid-state cyanine dye sensitized solar cells," *Journal of Materials Chemistry*, vol. 17, no. 29, pp. 3037–3044, 2007.

[14] D. Kavitha and C. Namasivayam, "Experimental and kinetic studies on methylene blue adsorption by coir pith carbon," *Bioresource Technology*, vol. 98, no. 1, pp. 14–21, 2007.

[15] M. Doğan, M. Alkan, Ö. Demirbaş, Y. Özdemir, and C. Özmetin, "Adsorption kinetics of maxilon blue GRL onto sepiolite from aqueous solutions," *Chemical Engineering Journal*, vol. 124, no. 1–3, pp. 89–101, 2006.

[16] N. Kannan and M. M. Sundaram, "Kinetics and mechanism of removal of methylene blue by adsorption on various carbons—a comparative study," *Dyes and Pigments*, vol. 51, no. 1, pp. 25–40, 2001.

[17] Y. S. Ho and G. McKay, "Pseudo-second order model for sorption processes," *Process Biochemistry*, vol. 34, no. 5, pp. 451–465, 1999.

[18] S. Mustafa, B. Dilara, K. Nargis, A. Naeem, and P. Shahida, "Surface properties of the mixed oxides of iron and silica," *Colloids and Surfaces A*, vol. 205, no. 3, pp. 273–282, 2002.

[19] JCPDS 01-071-1166 (Anatase).

[20] JCPDS 00-021-1276 (Rutile).

[21] E. M. McCash, "Adsorption and desorption," in *Surface Chemistry*, Oxford University Press, Oxford, UK, 2001.

[22] P. V. Messina and P. C. Schulz, "Adsorption of reactive dyes on titania-silica mesoporous materials," *Journal of Colloid and Interface Science*, vol. 299, no. 1, pp. 305–320, 2006.